A new High Performance Multisonar System for Fast Mobile Robots

Uwe D. Hanebeck and Günther Schmidt
Department for Automatic Control Engineering (LSR)
Technische Universität München
80290 München, Germany
Tel. 089-2105-8395, Fax 089-2105-8340
e-mail:{hnb,gs}@lsr.e-technik.tu-muenchen.de

Abstract— **A new type of actively sensing multisonar system for obstacle avoidance, localization and map updating in indoor environments has been developed. It is composed of 24 individual intelligent transmitter and receiver elements arranged on a horizontal plane around a fast motion platform. The physical sensor elements can be electronically configured for various types of task–directed and situation–adaptive virtual sensor arrays, for example, reliable measurement of wall orientation and distance or for tracking a walking person. The combination of virtual sensor data with a–priori information about the mission and the environmental situation permits the sensor system to keep up with the data rate requirements of fast mobile platforms. Experimental tests with the developed multisonar system demonstrate its improved perception capabilities compared to the state–of–the–art.**

I. Introduction

Ultrasonic sensor systems in mobile robot applications serve three main objectives: detecting collisions with unexpected, possibly mobile, obstacles, localizing known environmental structures and updating an internal map with previously unknown objects.
Several mobile robot applications of ultrasonic sensing systems have been reported. One class of systems use only one rotating Time–of–Flight sonar sensing device to obtain a 360^o scan of the environment [4]. The width of the sonar beam causes a blurred image. Attempts to narrow the beam by phased arrays [2] or horn constructions [3] have already been undertaken. Mechanical positioning makes these systems slow and inadequate for collecting data during fast motion. Another class consists of systems where several (20–30) separate Time–of–Flight sensors surround a robot. Fixed firing schemes independent of mission and situation are employed [7], [13], [6]. Undesired mutual influences of the sensors result in slow firing rates and make error correction algorithms necessary [1]. Crosstalk effects are eliminated by identifying and rejecting pulses received from other sensors. The fastest system known to the authors achieves a sampling interval of 60 ms for each sensor with a maximum range of 2.5 m [1]. The separate evaluation of sensors results in a low angular resolution. This complicates most tasks, like determining the vehicle's own position or the position of a moving obstacle. While the second class of systems tries to avoid crosstalk effects, another class takes advantage of these phenomena. Sparse sensor arrays are used and the characteristics of sound propagation are taken into account. This approach permits determining the normal directions of walls [10], [12] or the tracking of moving obstacles as in [8]. The need for mechanical aiming renders these systems too slow for the intended application.

Since our sensor is designed to be used with an omnidirectional locomotion platform, the sensor system itself should provide omnidirectional measurement capabilities. In addition, we expect it to perform several tasks simultaneously, for example, localizing the walls while reliably scanning the current travelling direction. Data has to be provided at a sufficiently high rate to guide a fast (2 m/sec) mobile robot with steering commands generated every 10 msec. The maximum range should be adapted to indoor requirements, i.e. up to 4 m. Furthermore the system should be inexpensive and to a large degree comprising commercially available components. The proposed system which combines useful aspects of today's systems is presented in detail in Section II. It is shown, how to dynamically build up heterogeneous sensing arrays dedicated to special tasks while in operation. A method to alleviate complicated cross–talk error correction schemes is presented. High–frequency firing schemes compensate for the slow speed of sound in air. Section III presents algorithms for extracting relevant environmental features with the proposed system. Section IV discusses the current prototypical implementation. Experiments with the multisonar system mounted on a fast motion platform are described in Section V. Compared to state–of–the–art systems our approach demonstrates improved perception capabilities that relieves subsequent algorithms like obstacle avoidance and localization substantially.

II. System Overview

The fast motion platform under consideration is designed for operation in a moderately structured indoor environment. Walls, doors and fixtures are known and stored in an internal 3D–map, where attributes like the type of material may be included. The ultrasonic sensor system takes advantage of a simple 2D–map which models the environment by closed polygons and circular arcs. The 2D–map is obtained by applying an appropiate transformation to the 3D–map.

Roving around, the robot perceives two types of geometric sensor data: data resulting from known static objects included in the map and data from unknown obstacles that may be static or moving. While constantly monitoring its position — either absolute with respect to a reference frame or relative with respect to certain structures — it encounters the first class of objects more frequently. Sampling schemes that take advantage of this prior knowledge are preferred. Information about the normal direction of walls simplifies the localization procedure.

Unknown objects must be detected to avoid collisions in the first place. With this in mind, it is desirable to prevent the robot from slowing down or even stopping due to spurious obstacles and other artifacts. On the other hand, it may be reasonable to expand the internal map for unknown static obstacles. To assist the vehicle pilot in deciding which direction to take, a moving obstacle has to be tracked, its velocity estimated, and its future path of motion predicted. The sampling interval of a fast (2 m/sec) mobile robot's locomotion control scheme is around 10 msec. Information should be provided at a comparable rate to ensure safe driving based on the ultrasonic sensor system.

A. *Dynamic reconfiguration*

24 transmitter and receiver elements arranged on a horizontal plane around a fast mobile robot constitute a homogeneous multisonar system. However, they are combined to form a variety of virtual sensing arrays adapted to different tasks and situations. This type of operation is similar to a concept described in [5]. Virtual sensors are aimed electronically, there is no need for moving parts.

One particular virtual sensor is dynamically formed as an array of adjacent sensors with one single transmitter and several receivers. This is especially useful when localizing linear structures common in the considered szenarios. Ultrasonic power emission is minimized which in turn reduces the overall measurement noise.

B. *Method of Virtual Point Source*

Moving with high speed in a busy hallway requires early detection of the nearest unknown obstacles and the determination of their positions. Usually several sensors are used separately for this purpose in Time–of–Flight mode. Disturbing crosstalk effects require elaborate error correction schemes.

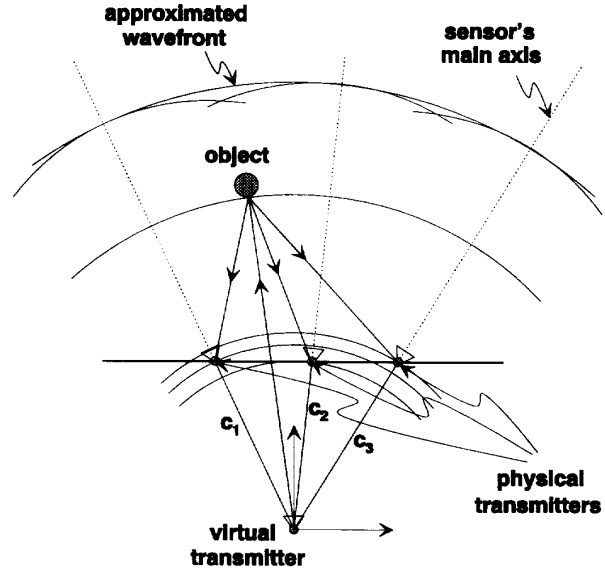

Figure 1: Combining sensors to form a virtual transmitter.

A more useful configuration for this would be one single transmitter with the desired beam form and a receiving array made up of several receivers in order to evaluate the incoming echos as reported in [8]. Since the considered vehicle may proceed in any direction, the transmitter would normally have to be rotated mechanically. Using the concept of dynamical reconfiguration, a virtual transmitter with the desired characteristics is obtained by appropiately phasing adjacent transmitters, Fig. 1. When it comes in contact with a physical transmitter, an imaginary circular wave, which is emanated from the origin, triggers a pulse. Depending on the desired beam width, several neighbouring sensors are employed. Since the sensors' main axes intersect at the origin, the respective pulses superpose to approximate the pulse of a single central transmitter.

Since we assume there is only one single pulse stemming from the origin, it is not necessary to decide which physical transmitter produced the pulse detected by an individual receiver. Rotating the beam to another focus of attention is achieved by shifting the arrangement electronically.

C. *Fast Firing*

It is common engineering practice to concentrate on a certain interval around a nominal or expected value. We could use prior knowledge from a map in conjunction with

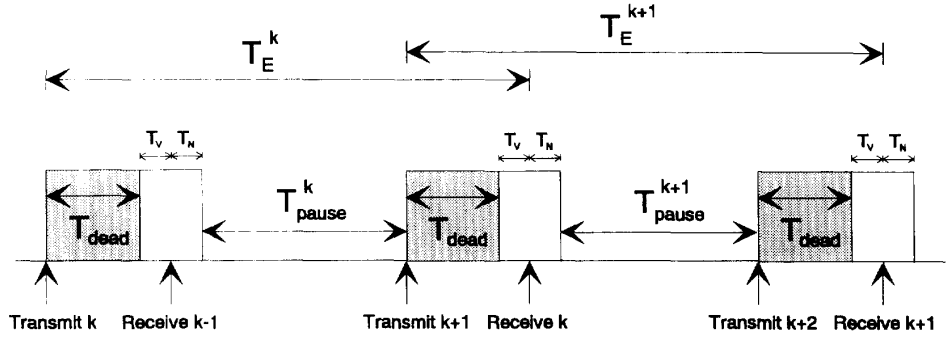

Figure 2: Fast firing — combining windowing and interlacing.

an estimated approximate position to a–posteriori discard inconsistent measurements. However, we propose to go one step further and use prior knowledge at an earlier stage, i.e. during the data gathering process and can receive echos only in certain unmasked timeslots that have been precalculated. This scheme is also applicable to reflectors not represented in the map. *Windowing* is then applied by predicting the distance to be measured from previous data. Missing an obstacle occluding the expected reflector is impossible because the firing scheme is changed when the predicted time-slot is empty for several times. Due to the slow speed of sound in air, the elapsed time between transmitting a pulse and receiving the returned echo is approximately 3 msec per meter travelled. With longer distances, *interlaced transmitting and receiving* becomes more and more appropiate.

Windowing and interlacing is combined in an effective manner. After initializing with a standard firing method, i.e. determining the expected echo return time T_E^k, we receive the echo from the previous pulse after the next one has been transmitted. A window of length $T_V + T_N$ ($T_V = T_N$) is centered around the expected time of arrival. The most straightforward scheme for one sensor is shown in Fig. 2. The pause time T_{pause}^k is calculated as

$$T_{pause}^k = T_E^k - 2 \cdot T_{dead} - 2 \cdot T_V - T_N \,. \tag{1}$$

The expected echo return time T_E^k is updated with the knowledge from every new sample $k-1$. T_{dead} corresponds to the dead zone, cf. Section IV. It is approximately 1.5 msec. T_V, T_N are set at around 0.5 msec. A high firing rate $1/T_s$, given by

$$\begin{aligned} T_s &= T_E - T_{dead} - T_V & (2)\\ &\approx \frac{d}{m} \cdot 6\,\text{msec} - 2\,\text{msec} & (3) \end{aligned}$$

is achieved, Fig. 3. d is the distance in m. We define the order of the fast firing scheme as being the number of pulses interlaced in the pause times. Keeping pace with the locomotion controller, a sampling frequency of 100 Hz

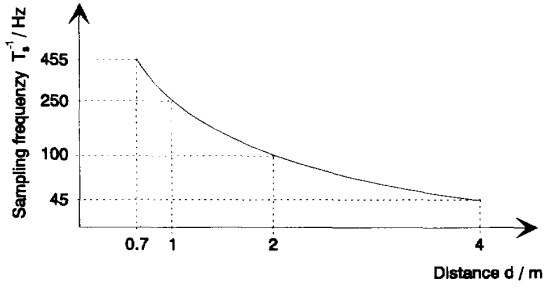

Figure 3: Sampling frequency for fast firing of first order as a function of distance.

is achieved with simple first order fast firing up to distances of 2 m. Thanks to windowing, the scheme is invulnerable to noise and secondary reflections. It is applicable for distances greater than approximately 70 cm; equivalent to times of flight greater than $2 \cdot T_{dead} + 2 \cdot T_V + T_N$. If the tracking process breaks down because the object is moving too fast, we restart with initialization measurements. In practice, a more refined scheme outside the scope of this paper is used. Fast firing of higher order is achieved by interlacing more pulses during the pause times.

III. Feature Extraction

With the concept of dynamic reconfiguration we build up virtual sensors from several transmitters/receivers and position them electronically where appropiate. In general, we use a virtual point source located at the vehicle's origin and an array of non–equally spaced receivers. Our goal is not only to obtain distance, but also to provide angular information about the extracted surface primitive. For this purpose let us consider a part of such an array consisting of one virtual transmitter and two receivers.

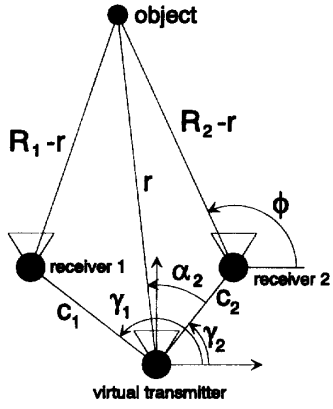

Figure 4: Point type reflector.

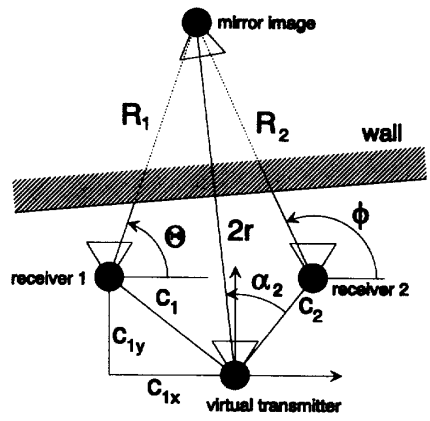

Figure 5: Wall reflector.

A. *One virtual transmitter / two receivers*

In [10] a system consisting of one transmitter and two receivers mounted on a rotating platform is introduced and an approximate solution for calculating the wall orientation is given. In [12], an analytic solution has been derived for an array consisting of one transmitter/receiver and two separate receivers mounted on the shafts of independently controlled stepper motors. We extend these concepts to our configuration and consider two types of reflector surface patches that are represented by i) points, i.e. edges and thin rods ii) straight line segments. With R_i the sum of the distances from sender to object and from object to receiver i, the first case is depicted in Fig. 4. The position of the point reflector is obtained by calculating the intersection of two ellipses. Each ellipse is defined by the transmitter which acts as common focal point and then by receiver 1 and 2 as the second focal point. Exact solutions are derived in the appendix and stated for reference in the following:

$$r = \frac{-B + \sqrt{B^2 - 4AC}}{2A} \tag{4}$$

$$\alpha_2 = \operatorname{acos}\left(\frac{r - p_2}{re_2}\right) \tag{5}$$

$$A = 1 - 2\frac{e_1}{e_2}\cos(\gamma) + \frac{e_1^2}{e_2^2} - e_1^2\sin^2(\gamma) \tag{6}$$

$$B = 2\left(-p_1 + \frac{e_1}{e_2}(p_1 + p_2)\cos(\gamma) - p_2\frac{e_1^2}{e_2^2}\right) \tag{7}$$

$$C = p_1^2 - 2\frac{e_1}{e_2}p_1p_2\cos(\gamma) + p_2^2\frac{e_1^2}{e_2^2} \tag{8}$$

$$p_i = \frac{R_i^2 - c_i^2}{2R_i},\ \gamma = \gamma_1 - \gamma_2 \tag{9}$$

$$e_i = \frac{c_i}{R_i},\ i = 1, 2. \tag{10}$$

The model may easily be extended to include cylindrical objects with non–zero radius R_0. A much simpler solution is obtained when the transmitter and the receiver are clustered together, i.e. $c_2 = 0$. In this case:

$$r = \frac{R_2}{2},\ \phi = \operatorname{acos}\left(\frac{R_2^2 - R_1R_2 + d^2}{R_2d}\right). \tag{11}$$

The second case is shown in Fig. 5. Assuming specular reflection, we use the mirror image method for obtaining wall distance and orientation. For details see appendix.

$$r = \frac{1}{2}\sqrt{c_1^2 + R_1^2 + 2R_1(c_{1x}h + c_{1y}\sqrt{1 - h^2})} \tag{12}$$

$$\alpha_2 = \operatorname{acos}\left(\frac{4r^2 + c_2^2 - R_2^2}{4rR_2}\right) \tag{13}$$

$$h = \frac{R_1^2 + d^2 - R_2^2}{2R_1d} \tag{14}$$

For the special case $c_2 = 0$, we obtain:

$$r = \frac{R_2}{2},\ \phi = \operatorname{acos}\left(\frac{R_2^2 - R_1^2 - d^2}{2R_2d}\right). \tag{15}$$

B. *One virtual transmitter / N receivers*

In the previous section we considered only part of an array and assumed the reflector type to be known a–priori with no ambiguities. However, at least three receivers are needed to discriminate objects like edges, planes, cylinders and to avoid misinterpretation. The differences between the arrival times define the incoming wave's curvature and therefore are the basis for a decision procedure. This decision process is sensitive to small errors in the measured

distances, thus yielding several misinterpretations in the straightforward scheme used in the experiments. A more robust scheme in conjunction with hardware modifications is currently being developed.

IV. Implementation Issues

The ultrasonic sensor units used in this project consist of state-of-the-art piezo-ceramic emitter and receiver elements. They operate at 40 kHz and are closely mounted together in a common housing. Each sensor may be activated at any point in time and switched to an *active* or *passive mode*. In *active mode* it operates as a sender, in *passive mode* it just listens. The maximum range is about 4 m for most reflectors which is sufficient for the intended applications. The minimum range — the dead zone — is approximately 25 cm due to masking the receiver shortly after transmitting a signal. 24 sensors are fixed on a horizontal plane around the mobile platform. To allow easy adjustment of azimuth and elevation during calibration they can be moved laterally and are cardanically attached. Each sensor is connected to an analog signal processing unit which creates pulses and detects the returned echos. A tandem-arranged digital signal processing unit determines the elapsed time between transmitting a pulse and for the echos to return. When converting the Times-of-Flight to distances, digitized values of temperature sensors are taken into account. The evaluation units are fully decoupled. A local transputer network consisting of four T805 transputers with the digital electronics mapped to memory executes configuration, the sensor firing, data gathering, and prefiltering. Transputers are high-performance computing devices that combine microcontroller-like capabilities (built-in timers, on-chip RAM) with number-crunching ($\approx$ 1 MFlops for T805/30). They provide four on-board, high-speed, bidirectional serial links (20 MBit/s) that work independently of the main processor. This simplifies the construction of multiprocessor systems. On this network concurrent processes are run, resulting in a decentralized control scheme which allows exact timing and a quick examination of the sensor status, i.e. when a signal is returned. This local intelligence is connected to the central transputer network of the mobile platform via four links, Fig. 6. The activities described so far are performed by the local intelligence and are transparent to users. A local expert module decides when to use which type of firing method by analyzing the current environmental situation, the estimated position and the actual requirements. The proposed system has been implemented in the form of communicating sequential processes (CSP) on the local transputer network. Synchronization and communication occurs via communication paths called channels. Developed as a research tool, the system provides enough computing power to be programmed at a high level. Students assisting in the project

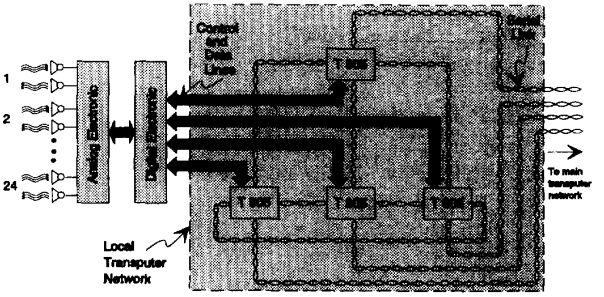

Figure 6: Overview ultrasonic sensing hardware.

do not have to bother with assembly language programming to achieve desired performance. Each sensor is controlled by a CSP and other CSPs are dedicated to system synchronization, configuration, and data collection. Due to the regular structure of the sensor system this implementation simplifies the development of algorithms when compared with writing one sequential program performing the same task. The software network is mapped on the hardware network consisting of four transputers.

V. Applications

ROMAN is a service robot with dimensions (width 63 cm x depth 63 cm x height 100 cm) accommodating indoor requirements, Fig. 7. Three independently steerable wheel systems provide excellent maneuverability. Wheel diameters of 20 cm allow travel across critical surfaces like carpeted floor. To simplify the construction, dead-reckoning is based on the drive wheels. No separate measurement wheels are supplied. The maximum speed of 2 m/sec has been chosen to correspond with human walking speeds and wheel-chair velocities. The sampling interval of the low-level motor control is 400 μs, steering commands are emitted every 10 msec based on actual position information. A lightweight 7 DOF manipulator with a maximum range of 80 cm is mounted in one corner of the platform. The computer architecture is based on a VMEbus. The main sensor system is operated by a distributed transputer network and consists of the ultrasonic sensors, the wheel based dead-reckoning system and a simple gyroscope. The network is connected to the VMEbus via a high-speed bridge. Including sensors, analog devices, digital hardware and the computing resources, the multisonar system occupies a 15 cm layer within ROMAN. The dead-reckoning system and the gyroscope are used to correct errors resulting from the vehicle's motion and to allow multiple view points.

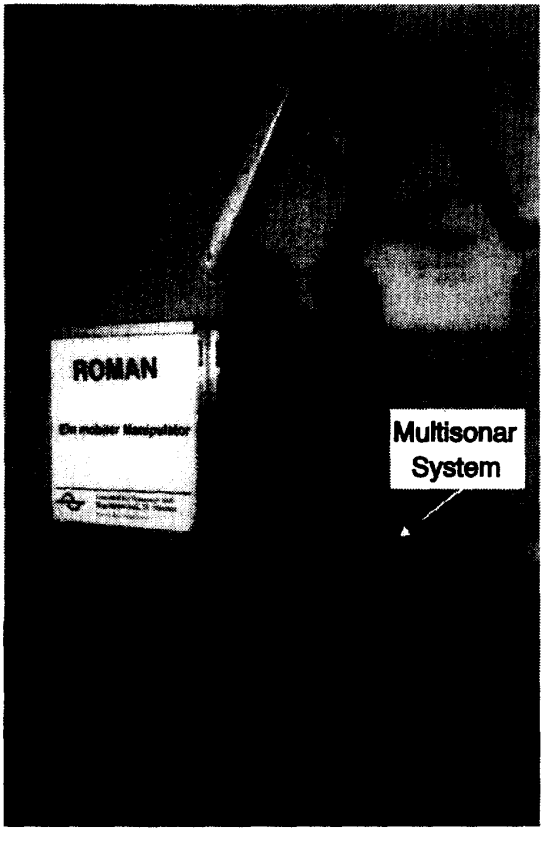

Figure 7: Mobile manipulator ROMAN.

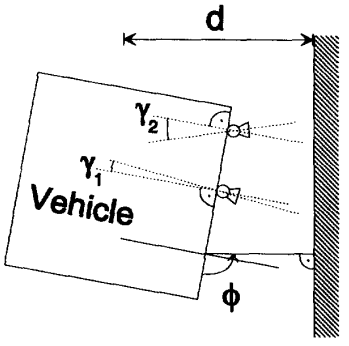

Figure 8: Experiment for determining wall orientation.

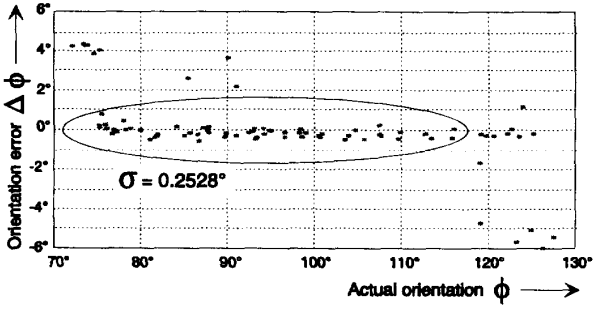

Figure 9: Results of determining the orientation of a wall.

A. *Determining wall orientation*

To demonstrate the performance of the algorithms described so far, the robot is positioned in front of a wall with randomly chosen orientations at an approximate distance of 1 m, Fig. 8. Real orientations are determined by manual reference measurements. When collecting samples, only two ultrasonic sensors, which have been separated by 91 mm are used without any support from other sensor systems. The sending sensor is oriented at an angle $\gamma_1 = 2°$ while the receiver is at $\gamma_2 = 15.5°$, Fig. 8. The error between actual and estimated orientation is shown in Fig. 9 as a function of the actual orientation. Between 75° and 115° the maximum absolute error is around 0.5° save three outliers. These may be due to errors in the manual reference determination, which is itself a high variance process. Outside of this interval the assumptions made are not applicable, leading to severe outliers. The absolute error's standard deviation is 0.2528^0. In the next experiment, encountering walls outside of the high confidence interval leads to repositioning of the virtual orientation sensor, i.e. shifting the responsibility to neighboring sensors. Fusing this information with data from dead-reckoning and the gyroscope results in a reliable basis for subsequent wall-following and localization algorithms.

B. *Map building*

Building a map of unknown obstacles while localizing a-priori known structures is demonstrated in the next experiment. Fig. 10 depicts the experimental environment. Two virtual sensors, each consisting of one collocated sender/receiver and a second receiver are used to determine the wall orientations. Via dynamic reconfiguration, they are positioned optimal to the walls. While travelling on the shown path, walls 1 and 3 are used at first as a localization reference. Sensors 21 and 22 monitor the distance and the orientation of wall 3 at all times. At switch point, sensors 15 and 16 become uncertain when measuring wall 1. Sensors 18 and 19 are employed next to measure wall 2 on the remaining path to the goal. This approach of using prior knowledge ensures a high ratio of reliable measurements compared to ultrasonic power emission. Fast firing is employed to achieve desired data rates.

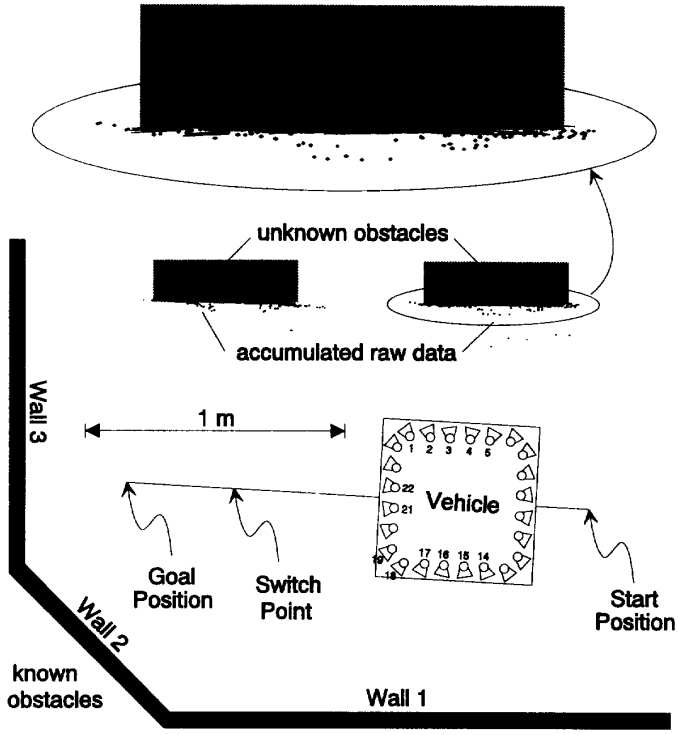

Figure 10: Map–building experiment.

In this experiment, simple fast firing of first order provides position information with a sampling interval less than 10 ms, cf. Fig. 3. This is sufficient for feeding the locomotion controller at its sampling rate of 100 Hz. Echos associated with obstacles known from the map are not depicted in Fig. 10.

To calculate the actual position estimate, the previous position is propagated via dead–reckoning and gyroscope and fused with actual ultrasonic measurements. The respective uncertainties are modeled with set–theoretic considerations. Statistical modeling would not capture the systematic errors occuring in conjunction with coordinating the three wheels. According to this point of view, the fusing process results in set intersection [11]. Going into more detail would take us too far afield.

Parallel to the localization task, sensors pointing in the appropiate direction are used for map–building. Edge and wall reflections are discriminated and the reflector positions are obtained with respect to the vehicle frame. Via the known transformation vehicle/world, raw data is plotted in world coordinates, Fig. 10. The exaggerated clipping reveals the performance of both obstacle detection and localization. Edges are marked by dots and wall surface patches are represented by a short line segment indicating their orientation. The achieved precision is the same as in the previous experiment. The additional surface information on each patch eases the determination of line endpoints and outlier refusal for subsequent segmentation algorithms. The decision edge/wall used here is sensitive to errors in the measurement process and several misinterpretations are visible in Fig. 10. Robustifying this decision process by modification of hardware and algorithms is the topic of current research. Conventional ultrasonic systems tend to narrow openings as the one in the experiment. In contrast to this, line segments extracted by the proposed system reliably cover the object surface. There are only some outliers classified as edges.

VI. Conclusions and Future Directions

A new high performance multisonar system for fast (2 m/s) omnidirectional mobile robots has been developed. 24 transmitter and receiver elements are arranged on a horizontal plane around a mobile robot and constitute a homogeneous construction set for transmitting and receiving arrays. Depending on mission and situation the individual elements are combined to form several heterogeneous virtual sensing arrays, each designed to carry out a given task. Aiming these virtual sensors is done electronically, there is no need for moving parts. High frequency

firing schemes exploit a–priori information about the current environment to purposefully collect data in a surveillance area of 8.6 meters in diameter. This makes our system superior to those with fixed data gathering schemes. An experiment has been described which underlines the system's perception capabilities when determining the orientation of walls. A maximum absolute error of 0.5^0 has been achieved. The second experiment has demonstrated the map–building of unknown obstacles while providing position information about known environmental structures at least at the locomotion controller's sampling rate of 10 ms.

References

[1] Borenstein, J. and Koren, Y., "Noise rejection for Ultrasonic sensors in Mobile Robot Applications". *Proceedings of the 1992 IEEE International Conference on Robotics and Automation, Nice, France*, S. 1727–1732, May 1992.

[2] Burks et al., "Autonomous Navigation, Exploration, and Recognition Using the HERMIES IIB Robot". *IEEE Expert*, Vol. 2, No. 4, S. 18–27, 1987.

[3] Crowley, J. L., "Dynamic world modelling for an intelligent mobile robot using a rotating ultrasonic ranging device". *Proceedings of the 1985 IEEE International Conference on Robotics and Automation, St. Louis, MO*, 1985.

[4] Drumheller, M., "Mobile Robot Localization Using Sonar". *IEEE Transactions on Pattern Analysis and Machine Intelligence*, Vol. 9, No. 2, S. 325–332, 1987.

[5] Fukuda, T. and Nakagawa, S., "Dynamically reconfigurable robotic systems". *Proceedings of the 1988 IEEE International Conference on Robotics and Automation, Philadelphia, PA*, S. 1581–1586, 1988.

[6] Holenstein, A. A. and Badreddin, E., "Collision Avoidance in a Behaviour–based Mobile Robot Design". *Proceedings of the 1991 IEEE International Conference on Robotics and Automation, Sacramento, CA*, S. 898–903, 1991.

[7] Kortenkamp et al., "Integrated Mobile–Robot Design, Winning the AAAI '92 Robot Competition". *IEEE Expert*, Vol. 8, No. 4, S. 61–73, 1993.

[8] Kuc, R. and Barshan, B., "Bat–Like Sonar for Guiding Mobile Robots". *IEEE Control Systems Magazine*, Vol. 12, No. 4, S. 4–12, 1992.

[9] Kuc, R. and Siegel, M. W., "Physically Based Simulation Model for Acoustic Sensor Robot Navigation". *IEEE Transactions on Pattern Analysis and Machine Intelligence*, Vol. 9, No. 6, S. 766–778, 1987.

[10] Nagashima, Y. and Yuta, S., "Ultrasonic sensing for a mobile robot to recognize an environment – Measuring the normal direction of walls –". *Proceedings of the 1992 IEEE/RSJ International Conference on Intelligent Robots and Systems, Raleigh, NC*, S. 805–812, July 7–10, 1992.

[11] Sabater, A. and Thomas, F., "Set Membership Approach to the Propagation of Uncertain Geometric Information". *Proceedings of the 1991 IEEE International Conference on Robotics and Automation, Sacramento, CA*, S. 2718–2723, 1991.

[12] Sabatini, A. M., "Active Hearing for External Imaging Based on a Ultrasonic Transducer Array". *Proceedings of the 1992 IEEE/RSJ International Conference on Intelligent Robots and Systems, Raleigh, NC*, S. 829–836, July 7–10, 1992.

[13] Walter, S. A., "The Sonar Ring: Obstacle Detection for a Mobile Robot". *Proc. IEEE International Conference on Robotics and Automation, Rayleigh, NC, March 31. - April 3.*, S. 1574–1579, 1987.

Appendix

In Fig. 4 two ellipses are defined by

$$r = \frac{P_i}{1 + e_i \cos(\alpha_i)}\,,\ i = 1, 2 \tag{16}$$

$$\alpha_1 + \alpha_2 = \gamma_1 - \gamma_2 = \gamma\,. \tag{17}$$

With Eqns. (16), 17) we obtain

$$r\{1 - e_1[\cos(\gamma)\cos(\alpha_2) + \sin(\gamma)\sin(\alpha_2)]\} = p_1 \tag{18}$$

$$\cos(\alpha_2) = \frac{r - p_2}{re_2} \tag{19}$$

$$\sin(\alpha_2) = \frac{\sqrt{r^2(e_2^2 - 1) - 2rp_2 + p_2^2}}{re_2}\,. \tag{20}$$

Plugging Eqns. (19),(20) into Eqn. (18) results in a quadratic equation for r

$$Ar^2 + Br + C = 0 \tag{21}$$

with coefficients stated in Section III.
For a wall type object as in Fig. 5 we conclude that

$$\cos(\theta) = \frac{R_1^2 + d^2 - R_2^2}{2R_1 d} = h\,. \tag{22}$$

The position of the mirror image is found as

$$x_{MI} = c_{1x} + R_1\cos(\theta) \tag{23}$$

$$y_{MI} = c_{1y} + R_1\sin(\theta)\,. \tag{24}$$

The distance r is then

$$r = \frac{1}{2}\sqrt{x_{MI}^2 + y_{MI}^2} \tag{25}$$

and α_2 is given by

$$\alpha_2 = \operatorname{acos}\left(\frac{4r^2 + c_2^2 - R_2^2}{4rR_2}\right)\,. \tag{26}$$